Optimizing Joint Speed and Altitude Schedule for UAV Data Collection in Low-Altitude Airspace

Addressed Comments for Publication to

IEEE Transactions on Mobile Computing

by

Yiqian Wang, Jianping Huang, Feng Shan, Yuming Gao, Runqun Xiong and Junzhou Luo

Dear editors,

Please find enclosed the revised version of our previous submission entitled "Optimizing Joint Speed and Altitude Schedule for UAV Data Collection in Low-Altitude Airspace" with manuscript number TMC-2025-02-0445. We would like to thank you and the reviewers for the valuable comments which help improving the quality of our manuscript. In this revision, we have carefully addressed the reviewers' comments. A summary of main modifications and a detailed point-by-point response to the comments from Reviewers 1 and 3 (following the reviewers' order in the decision letter) are given below.

Sincerely,

Yiqian Wang, Jianping Huang, Feng Shan, Yuming Gao, Runqun Xiong and Junzhou Luo

Note: To enhance the legibility of this response letter, all the editor's and reviewers' comments are typeset in boxes. Rephrased or added sentences are typeset in color. The respective parts in the manuscript are highlighted to indicate changes.

Response to the Meta Review

Response S1: We appreciate your handling of the review process.

According to the reviewers' comments, we have checked our manuscript and addressed them in the following way:

1. We added content.

2. We removed our wrong statements in Section I.

Response to Reviewer 1

Comment 1.1

This paper fails to justify the selection of heuristic factors (α, β) in SSF-ACO. You should conduct grid search experiments to demonstrate parameter sensitivity or cite theoretical foundations for ACO parameter tuning.

Response 1.1:

Thank you for the comment. We performed a grid-search over representative combinations of the pheromone exponential factor $\alpha \in \{1, 2, 3, 4\}$ and heuristic exponential factor $\beta \in \{0, 1, 2, 3, 4\}$ to access parameter sensitivity as shown in Figure 1. The algorithm's performance under $\beta = 0$ is significantly worse than performance for other parameter combinations. $\beta = 0$ eliminates the use of heuristic information, resulting in purely random exploration during the initial iterations and thus poor performance. The results also indicate that the configuration $\alpha = 1, \beta = 2$ consistently achieves the minimum energy consumption. Accordingly, we adopted $\alpha = 1, \beta = 2$ in all simulation experiments.
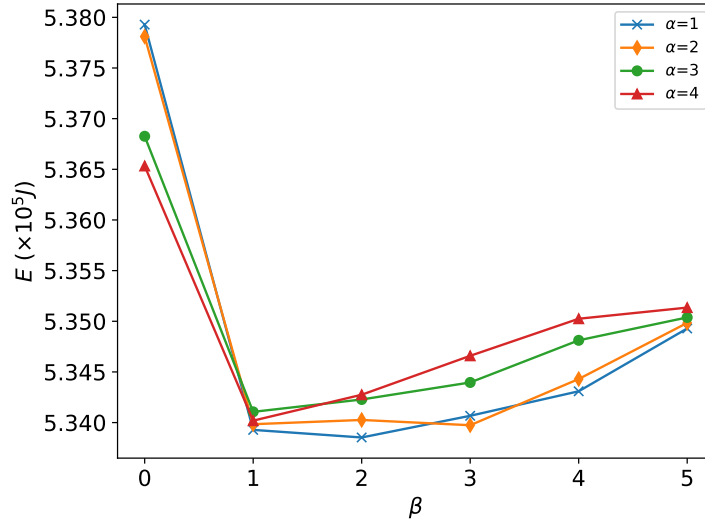

Figure 1: Performance of SSF-ACO across different (α, β) combinations.

Comment 1.2

Current experiments only cover small-scale scenarios (≤ 30 nodes), it should extend to more nodes to should the scalibility of algorithm.

Response 1.2:

Thank you for the suggestion. Our algorithms are designed with scalability and is capable of handling larger-scale problems. To further verify its scalability, we extended the evaluation to include scenarios involving 35 and 40 ground sensor nodes. The updated results are illustrated in Figure 2, which is identical to Figure 8a in the manuscript. The results demonstrate that the proposed algorithms continue to exhibit superior performance even in larger-scale scenarios.
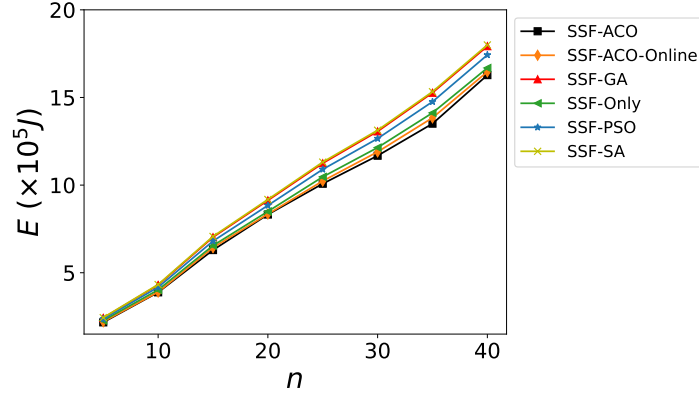
Figure 2: Algorithm performance comparisons in UAV energy consumption under varying numbers of sensors.

Comment 1.3

The assumptions of linear GN deployment and complete GN knowledge are restrictive and not sufficiently justified. Please provide a detailed discussion of the assumptions, including their implications for real-world applicability and potential extensions.

Response 1.3:

We appreciate the reviewer's comment regarding the assumptions of linear GN deployment and complete GN knowledge. We would like to provide additional details about GN deployment and GN knowledge, as well as a discussion of these assumptions in Section 6 of our revised manuscript.

Linear GN deployment. The linear configuration of GNs represents a reasonable and commonly utilized setup in real-world systems. This deployment pattern often arises in infrastructure monitoring scenarios. For instance, in the power line [1], [2], UAVs are dispatched to autonomously collect data from sensors on the transmission tower. Similarly, in the oil and gas industry [3], UAVs are used to fly along pipelines for inspection activities. In addition, sensors can be deployed along rivers [4] and coasts [5] to capture diel and seasonal fluctuations, with the purposes of ecological monitoring, flood warning, and scientific research.

In fact, the effectiveness of such linear GN deployment has already been demonstrated in industrial applications to reduce costs, improve work efficiency, and avoid hazardous manual tasks. For instance, DJI has successfully implemented UAV-enabled solutions in scenarios such as long-distance pipelines [6], power transmission line in plateau regions [7], and river ecosystems [8], where the UAV trajectories can be regarded as linear or the combination of multiple straight-line segments.

Complete GN knowledge. Sensor knowledge mainly includes information such as position, amount of data to be collected, transmission rate, and data transmission range. (1) In the online problem, each sensor has an additional control communication range, which covers a larger area than the data transmission range. When the UAV enters the sensor's control communication range, it can detect the sensor and receives a response containing information such as the amount of data and the sensor's position. (2) There is a proportional relationship between the radius of the data transmission range and the control communication range. Based on the distance between the sensor and the UAV at the moment the response is received, the radius of the data transmission range can be estimated. (3) The sensor position is fixed,

and thus, it can be obtained during the initial deployment and periodic maintenance. This allows for the calibration of sensor positions.

Discussion in the manuscript. We have extended the discussion of these assumptions in Section 6 of the revised manuscript as follows.

> The UAV keeps broadcasting 'Probe' message during the flight to detect sensors. Once receiving the 'Probe' message, the sensor sends back an 'ACK' message, which includes its position, the amount of data, and transmission characteristics. Note that each sensor sends 'ACK' message only once. This partial information availability fundamentally changes the nature of our optimization problem, requiring real-time decision-making based on local information.

Comment 1.4

Could the proposed models and algorithms be adapted for 3D GN layouts?

Response 1.4:

Thanks for your comment. Our current focuses on the linear (2D) GN distribution, including power transmission lines, roads, pipelines, river and coast. By integrating advanced trajectory planning methods, our algorithms can be extended to 3D GN layout.

Specifically, we first apply a trajectory planning algorithm to optimize the UAV's flight path and avoid collisions. The area of UAV trajectory planning and collision avoidance has been extensively studied in recent years. The distance travelled from the starting point to any location along the trajectory is treated as the horizontal coordinate of that location. Along this trajectory, we can then use SSF-ACO algorithm to jointly optimize speed and altitude scheduling.

Although promising, this approach to extending the 3D GN layout remains subject to certain limitations. Jointly optimizing the 3D trajectory and speed scheduling is expected to have a better performance. Furthermore, the increased computational complexity associated with 3D scheduling problems presents additional challenges. However, these issue fall within a broader area that extends beyond the focus of the current work. Addressing them remains also one of our future research directions. In this work we concentrate on the optimization of speed and altitude scheduling, and demonstrate compatibility with existing trajectory planning algorithms.

Comment 1.5

Some statements have inconsistent tenses (e.g. "Our previous work [20] investigated..."). vs. ("we propose..."), need to unify the full text tense; The reference format should be checked according to IEEE standards (e.g. URL references [6] are not standardized).

Response 1.5:

Thank you for the comment. We have carefully reviewed the tense usasge throughout the manuscript and corrected the inconsistent expressions to ensure consistency. Additionally, we have standardized the website reference format according to IEEE Reference Guide.

[1] B. Mendu and N. Mbuli, "State-of-the-Art Review on the Application of Unmanned Aerial Vehicles (UAVs) in Power Line Inspections: Current Innovations, Trends, and Future Prospects," *Drones*, vol. 9, no. 4, p. 265, 2025.

[2] Y. Luo, X. Yu, D. Yang, and B. Zhou, "A survey of intelligent transmission line inspection based on unmanned aerial vehicle," *Artif. Intell. Rev.*, vol. 56, no. 1, pp. 173–201, 2023.

[3] L. C. Sousa, Y. M. R. da Silva, G. G. R. de Castro, *et al.*, "Autonomous Path Follow UAV to Assist Onshore Pipe Inspection Tasks," in *2022 7th Int. Conf. Robot. and Automat. Eng. (ICRAE)*, IEEE, 2022, pp. 112–117.

[4] S. G. Burman, J. Gao, G. B. Pasternack, *et al.*, "TempMesh - A Flexible Wireless Sensor Network for Monitoring River Temperatures," *ACM Trans. Sen. Netw.*, vol. 19, no. 1, p. 28, 2022.

[5] T. Ahmed, L. Creedon, and S. S. Gharbia, "Low-Cost Sensors for Monitoring Coastal Climate Hazards: A Systematic Review and Meta-Analysis," *Sensors*, vol. 23, no. 3, 2023.

[6] DJI, *Pipeline Inspection - DJI Drone Solutions for the Oil and Gas Industry*, DJI Enterprise. Accessed Apr. 21, 2025. [Online]. Available: `https://enterprise.dji.com/cn/oil-and-gas/gathering-pipeline-inspection`.

[7] DJI, *The M300 RTK Excels in Plateau Power Line Inspection*, DJI Enterprise. Accessed Apr. 21, 2025. [Online]. Available: `https://enterprise.dji.com/cn/news/detail/m300-highland-power-patrol`.

[8] DJI, *Unmanned Aerial Vehicles Help the Environmental Management of Rivers in the Yangtze River Basin*, DJI Enterprise. Accessed Apr. 21, 2025. [Online]. Available: `https://enterprise.dji.com/cn/news/detail/yangtze-river-river-treatment`.

Response to Reviewer 2

Comment 2.1

The computational latency of SSF-ACO-Online needs justify.

Response 2.1:

Thank you for the suggestion. We have reported the cumulative computational time of SSF-ACO-Online and the corresponding UAV flight durations. These results are summarized in Table 1 (Table 4 in the manuscript) and discussed in the revised manuscript as follows to demonstrate the suitability of SSF-ACO-Online.

Table 1: Computation Time of SSF-ACO and SSF-ACO-Online Compared with UAV Flight Duration in Online Scheduling (in Seconds)

n	5	10	15	20	25	30	35	40
T_f	513.73	1107.11	1502.68	2084.67	2675.47	2997.83	3519.72	4119.79
T_{off}	1.58	5.60	12.01	19.11	32.32	51.01	64.60	92.73
T_{on}	0.99	1.81	2.91	3.09	3.49	3.87	5.04	5.80
T_{on}/T_f	0.19%	0.16%	0.19%	0.15%	0.13%	0.13%	0.14%	0.14%

> Finally, we analyze the computational latency of SSF-ACO-Online. Table 4 reports the duration of UAV flights T_f under online problem, along with the computation time of SSF-ACO-Online T_{on}, and that of SSF-ACO T_{off} in the corresponding offline problem. Across varying numbers of sensors, the computation times of SSF-ACO-Online stay under 6 seconds and constitute no more than 0.19% of the corresponding UAV flight duration. This demonstrates the suitability of SSF-ACO-Online for online applications. Since the active sensor list only maintains those sensors that have been discovered but not yet completely collected, though invoked SSF-ACO multiple times, SSF-ACO-Online has a cumulative computation time significantly shorter than that of SSF-ACO.

Comment 2.2

Alg. 4 does not specify the specific implementation of "Roulette-Wheel-Selection", which needs to supplement pseudocode or reference standard methods.

Response 2.2:

Thanks for your suggestion. The classic Roulette wheel selection method is applied, and we have added a brief description of the Roulette-Wheel-Selection method in the revised manuscript as follows.

> Specifically, in **Roulette-Wheel-Selection**, vertex $(\varphi + 1, j')$ is selected if $\sum_{j''=0}^{j'-1} P_{\varphi,j,j''}^{sel} \leq$ rand() $< \sum_{j''=0}^{j'} P_{\varphi,j,j''}^{sel}$, where rand() generates a random number in $[0, 1)$.

The vertical energy consumption is assumed to be linear related to the altitude difference, which seems oversimplified, more justification is needed.

Response 2.3:

Thanks for the comment. We would like to clarify that the proposed algorithm is applicable to arbitrary forms of vertical energy consumption models to achieve more accurate energy estimations. The "linear assumption" adopted in the manuscript is intended solely to simplify computations and to maintain focus on the problem under study, rather than to deliberately obtain more favorable results. We have added an explanation to the revised manuscript.

> Note that the proposed algorithm in Section 5 is applicable to more accurate vertical energy consumption models, and such assumption is only used to simplify computations.

Moreover, research [1] serves as the theoretical basis for this "linear assumption". According to [1], the following equation fits well with the theoretical derivation,

$$p_v = c_{0,v} + c_{1,v} v + c_{2,v} v^2, \tag{1}$$

where p_v is the vertical power consumption, $c_{0,v}$, $c_{1,v}$ and $c_{2,v}$ are coefficients, and v is the climbing or descending speed of the UAV. In our manuscript, we assume that the UAV climbs or descends at a constant speed and flies in a stable environment. Therefore, the vertical power consumption is constant. For a certain altitude difference Δh, the vertical energy consumption is $E_v = \frac{p_v \Delta h}{v}$, which supports the "linear assumption". Furthermore, similar assumptions have also been adopted in previous research [2].

The difference between the transmission range model of Equation (17) and literature [35] is not fully explained, and the improvement points or advantages need to be clearly defined.

Response 2.4:

Thanks for the comment. In [3], the probability of LoS link is considered as a continuous function of elevation angle θ. However, we use Eq. (2) to represent this radius-altitude relationship as a deterministic coverage abstraction, rather than as a probabilistic function. We have revised the manuscript to clarify the motivation for employing this equation.

> Based on the widely-used approximate funciton of LoS probability, the ground-to-UAV transmission range varies with flight altitude [3]. Higher altitudes expand the UAV's field of view, increasing the likelihood of establishing a LoS link. However, this also reduces the coverage radius. Here, we use Eq. (2) to represent this radius-altitude relationship

as a deterministic coverage abstraction, rather than as a probabilistic function:

$$\mu(\frac{x-x_0}{C_W}^2) + ((\frac{x-x_0}{C_W})^2 + (\frac{y}{C_H})^2)^2 \tag{2}$$
$$+ 2\frac{y}{C_H}((\frac{x-x_0}{C_W})^2 + (\frac{y}{C_H})^2) = 0,$$

where x_0 is the deployment position of the snesor, μ is the swell coefficient influencing the shape of the data transmission range. The width and height of the range are linearly related to the coefficients C_W and C_H, respectively. And the quantitave relationship can be found in Appendix F of the supplementary material. Although real-world sensor transmission ranges lack sharply defined boundaries, a deterministic coverage abstraction offers practical benefits by aligning with the radius-altitude variation trend and improving computational tractability.

Comment 2.5

What is the purpose of presenting Equation (18)?

Response 2.5:

Thans you for the comment. Equation (18) in the original manuscript was included to provide a quantitative description of the data transmission range's width. To retain a more holistic presentation, we have modified the expression.

> The width and height of the range are linearly related to the coefficients C_W and C_H, respectively. And the quantitave relationship can be found in Appendix F of the supplementary material.

Comment 2.6

There are too many curves in Figure 8 and the colors are similar, so it is difficult to distinguish them. It is suggested to optimize the color matching or add mark symbols

Response 2.6:

Thanks for your suggestion. We have revised the color scheme and marker symbols to make the curves in Figure 8 in the revised manuscript (Figure 3 in the following), and also adjusted the layout of it to improve clarity.

Comment 2.7

The dynamic nature of the sensor is not considered, such as movement, inaccurate position, failure and other problems.

Response 2.7:

We appreciate the reviewer's comment on the dynamics of sensors, which highlights important aspects that could influence the effectiveness the UAV scheduling. In the following,

(a) The number of sensors.

(b) The upper bound of coefficient of required time for data collection.

(c) The upper bound of height coefficient.

(d) The upper bound of width coefficient.

(e) The upper bound of swell coefficient of data transmission range.

(f) The finest granularity of altitude change for UAV.

(g) The vertical consumption coefficient.

(h) The radius ratio of the control communication range to the data transmission range of a sensor.
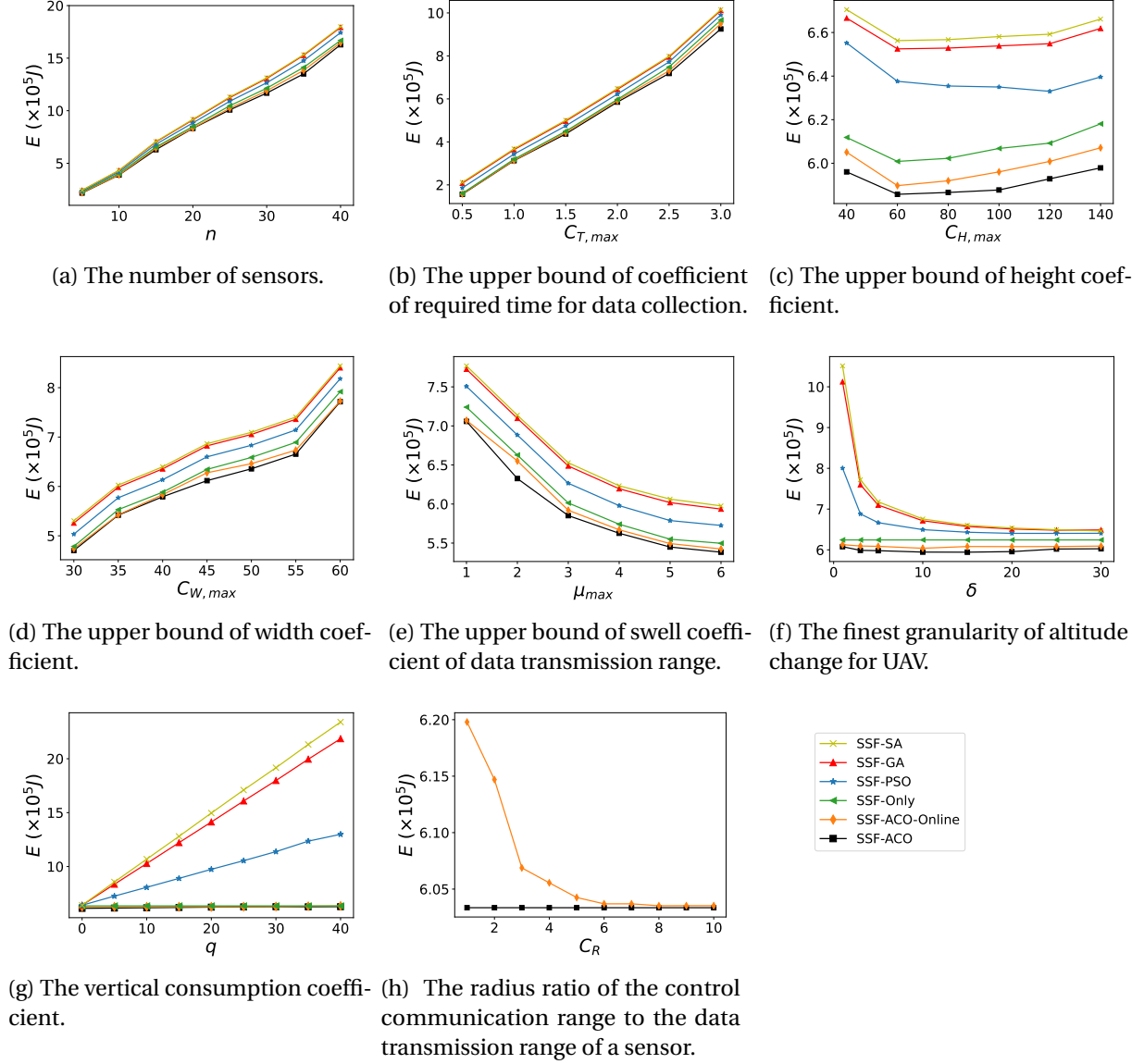
Figure 3: Algorithm performance comparisons in UAV energy consumption.

we will discuss the ground nodes (GNs) mobility, inaccurate position, failures, and unstable communication environment.

GN mobility. GN mobility is an important factor in various UAV-assisted systems. However, our current work focuses on data collection from stationary sensors. In the scenarios we consider, the sensors are fixed in the environment to monitor infrastructures or natural conditions. Admittedly, a number of existing studies [4]–[7] have investigated GN mobility. In these studies, GNs typically refer to mobile user devices with significant movement, such as user-carried devices [4], [5] or vehicles [6], [7], which are fundamentally different from the stationary GNs considered in our work.

Inaccurate position. The proposed algorithm relies on the precise sensor positions. However, the inaccurate sensor localization leads to discrepancies between the UAV scheduling and actual environment. In our future, we intend to employ more advanced relative positioning techniques to reduce localization inaccuracy and incorporate error-tolerant strategies to improve the system's robustness and reliability.

Failures. Failures may occur either before or during data transmission. Failures before transmission will result in the sensor being undetectable by the UAV. On the other hand, failures during the transmission process will lead to a disruption in the connection between the UAV and the sensor. The UAV will attemp to reconnect and, after reaching the maximum number of reconnection attempts, will abandon the connection. Regardless of whether reconnection is successful, the scheduling will be re-planned to ensure energy efficiency.

Unstable communication environment. The changes in the communication environment may lead to fluctuations in the transmission rate. When the UAV first detects the sensor, it will receive the sensor's guaranteed minimum transmission rate included the sensor's 'ACK' message. When the guaranteed transmission rate is not met, the UAV's speed and altitude scheduling will be re-planned by our algorithm to adapt to the environment changes.

Comment 2.8

Some minor suggestions:
(1) The the first sentence in subsection 2.1, "UAV" $\rightarrow$ "UAVs".
(2) Second paragraph of subsection 2.1, "maintaining" $\rightarrow$ "maintained".
(3) Second paragraph of subsection 2.2, "maintaining" $\rightarrow$ "and maintain".
(4) The "=" in table 1.
(5) Add $k \neq k'$ to equation (11), and $i \neq i'$ to equation (12).
(6) The parameter $\mathbb{S}$ of algorithm 1 and 2 is neither used nor updated.
(7) Line 2 of Algorithm 3, why set 20 to Z?

Response 2.8:

Thanks for your detailed suggestions. In response, we have made the following revisions.

For points (1) to (4), we have improved the phrasing and table in the manuscript to mamke it more consistent and easier to read.

For point (5), we would like to clarify that in Definition 1 in the manuscript, the condition $k < k'$ is defined. Additionally, in Equation (11), the condition $b_k < b_{k'}$ already implicitly ensures that $k \neq k'$. As for Equation (12), we have removed it along with its related content to improve the overall structure and clarity of the manuscript.

For point (6), $\mathbb{S}$ is defined as a data structure that encapsulates essential sensor information. To improve clarity and facilitate readers' understanding, we have revised the manuscript by relocating the description of $\mathbb{S}$ closer to Algorithm 1 and 2.

> For details, Alg. 1 takes the necessary sensor information as input and returns the optimal horizontal energy consumption. For simplicity, we denote these pieces of sensor information (such as l_i and r_i) by $\mathbb{S}$.

For point (7), we have added an explanation in the revised manuscript.

> Here, Z is set to 20 to balance solution quality and computational efficiency.

---

[1] K. Wu, M. Feng, C. Wu, Y. Lin, and S. Lu, "Trajectory Planning for Multi-rotor UAV Based on Energy Cost Model," in *2022 41st Chinese Control Conf. (CCC)*, IEEE, 2022, pp. 1–6.

---

[2] Y. Cao, A. Wang, G. Sun, and L. Liu, "Average Transmission Rate and Energy Efficiency Optimization in UAV-assisted IoT," in *2023 IEEE Wireless Commun. and Netw. Conf. (WCNC)*, IEEE, 2023, pp. 1–6.

[3] A. Al-Hourani, S. Kandeepan, and S. Lardner, "Optimal LAP altitude for maximum coverage," *IEEE Wireless Commun. Letters*, vol. 3, no. 6, pp. 569–572, 2014.

[4] L. He, G. Sun, Z. Sun, *et al.*, "An Online Joint Optimization Approach for QoE Maximization in UAV-Enabled Mobile Edge Computing," in *IEEE INFOCOM 2024 - IEEE Conf. Comput. Commun.*, IEEE, 2024, pp. 101–110.

[5] Z. Sun, G. Sun, L. He, F. Mei, S. Liang, and Y. Liu, "A Two Time-Scale Joint Optimization Approach for UAV-assisted MEC," in *IEEE INFOCOM 2024 - IEEE Conf. Comput. Commun.*, IEEE, 2024, pp. 91–100.

[6] X. Dai, Z. Xiao, H. Jiang, and J. C. S. Lui, "UAV-Assisted Task Offloading in Vehicular Edge Computing Networks," *IEEE Trans. Mobile Comput.*, vol. 23, no. 4, pp. 2520–2534, 2024.

[7] L. Fu, Z. Zhao, G. Min, W. Miao, L. Zhao, and W. Huang, "Energy-Efficient 3-D Data Collection for Multi-UAV Assisted Mobile Crowdsensing," *IEEE Trans. Comput.*, vol. 72, no. 7, pp. 2025–2038, 2022.

Response to Reviewer 3

Comment 3.1

Compared with previous works, the current work further considers the complex overlapping range relationship between sensors. Therefore, the authors should spend a lot of effort to emphasize this contribution in Section I.

Response 3.1:

Thanks for the valuable suggestion. We have revised Section 1 to better highlight the challenge introduced by this overlapping range relationship between sensors, and to underscore their practical relevance in real-world scenarios.

The revised description of this relationship:

> This altitude-dependent coverage creates intricate spatial relationships between sensors, manifesting in various overlapping patterns: partial overlap, full containment, reverse containment, and disjointness. Moreover, these relationships become even more complex as communication range changes with altitude, creating challenges that have not been fully addressed in previous research. For example, in Fig. 1, as the altitude increases, sensor S_1 initially overlaps with S_2, but eventually becomes fully contained by S_2. Such overlapping range relationship better captures the complexity of real-world scenarios and provides practical value for UAV-assisted data collection. Capturing and fully exploiting these altitude-dependent ranges is crucial, since it enables the data from a single sensor to be collected across multiple sessions and fundamentally influences the order of data collection.

The third challenge in the revised manuscript:

> Due to the complex overlapping patterns of sensor data transmission ranges, the UAV is often simultaneously located within the ranges of multiple sensors. Consequently, determining the optimal data collection sequence becomes highly challenging.

Comment 3.2

The system model assumes an idealized scenario without incorporating real-world path loss effects (e.g., fading, shadowing). This limits the practical use of the proposed algorithm.

Response 3.2:

Thank you for your comment. We have added Subsection 3.1.2 "Communication Model", where the probabilistic line-of-sight model is employed to model the communication between the UAV and sensors. The revised manuscript is shown below.

> The UAV collects data from sensors via sensor-to-UAV links. In this work, the probabilistic LoS channel model is employed [1] The channel coefficient H_i between the UAV

and sensor s_i at time t can be represented as follows:

$$H_i(t) = \sqrt{\beta_i(t)}\,\widetilde{H}_i(t), \tag{3}$$

where $\widetilde{H}_i(t)$ denotes the complex coefficient of small-scale fading with $E[|\widetilde{H}_i(t)|^2] = 1$, and $\beta_i(t)$ is the coefficient for the shadowing and path loss. Generally, $\beta_i(t)$ depends on LoS or non-LoS link condition [2],

$$\beta_i(t) = \begin{cases} \widetilde{\beta}/d_i^{\gamma}(t), & \text{LoS link,} \\ \kappa\widetilde{\beta}/d_i^{\gamma}(t), & \text{non-LoS link,} \end{cases} \tag{4}$$

where $\widetilde{\beta}$ reflects the path loss at unit distance, $d_i(t)$ represents the distance between the UAV and s_i, γ is the path loss exponent, and $\kappa \in (0, 1)$ captures the attenuation effect under the non-LoS conditions.

Let $P_i^{LoS}(t)$ be the LoS probability between the UAV and sensor s_i. The expectation of the channel power gain is given as follows [1]:

$$E[|H_i(t)|^2] = P_i^{LoS}(t)\frac{\widetilde{\beta}}{d_i^{\gamma}(t)} + (1 - P_i^{LoS}(t))\frac{\kappa\widetilde{\beta}}{d_i^{\gamma}(t)}. \tag{5}$$

Finally, the average transmission rate between the UAV and sensor s_i at time t can be given as [3]:

$$R_i(t) = B\log_2(1 + \frac{GE[|H_i(t)|^2]p_i}{N_0 B}), \tag{6}$$

where B is the bandwidth of the channel, G denotes the antenna gain, p_i denotes the transmission power, and N_0 represents the noise variance.

Comment 3.3

The claim of "near-optimal performance" for SSF-ACO-Online lacks a clear benchmark (e.g., theoretical bounds or exhaustive search). Provide a quantitative comparison to support this conclusion.

Response 3.3:

We appreciate the reviewer's insightful comment. We recognize that the term "near-optimal" was not precise. Our intention was to indicate that SSF-ACO-Online performs closely to the offline algorithm SSF-ACO. We have revised the abstract to clarify this point and removed the term "near-optimal" to avoid confusion.

Extensive simulations demonstrate that SSF-ACO significantly outperforms baseline approaches in energy efficiency, and SSF-ACO-Online achieves comparable performance with energy consumption 1.24% higher than offline counterpart in average.

The robustness of the SSF-ACO and SSF-ACO-Online algorithms to network dynamics (e.g., node mobility) is not evaluated. Include tests under time-varying conditions to demonstrate adaptability.

Response 3.4:

We appreciate the reviewer's comment on the network dynamics. The ground nodes (GNs) mobility, failures, and the computational latency of SSF-ACO-Online are discussed in the following.

GN mobility. GN mobility is an important factor in various UAV-assisted systems. However, our current work focuses on data collection from stationary sensors. In the scenarios we consider, the sensors are fixed in the environment to monitor infrastructures or natural conditions. Admittedly, a number of existing studies [4]–[7] have investigated GN mobility. In these studies, GNs typically refer to mobile user devices with significant movement, such as user-carried devices [4], [5] or vehicles [6], [7], which are fundamentally different from the stationary GNs considered in our work.

Failures. Failures may occur either before or during data transmission. Failures before transmission will result in the sensor being undetectable by the UAV. On the other hand, failures during the transmission process will lead to a disruption in the connection between the UAV and the sensor. The UAV will attemp to reconnect and, after reaching the maximum number of reconnection attempts, will abandon the connection. Regardless of whether reconnection is successful, the scheduling will be re-planned to ensure energy efficiency.

The computational latency of SSF-ACO-Online. We have reported the cumulative computational time of SSF-ACO-Online and the corresponding UAV flight durations. These results are summarized in Table 2 (Table 4 in the manuscript) and discussed in the revised manuscript as follows to demonstrate the suitability of SSF-ACO-Online.

Table 2: Computation Time of SSF-ACO and SSF-ACO-Online Compared with UAV Flight Duration in Online Scheduling (in Seconds)

n	5	10	15	20	25	30	35	40
T_f	513.73	1107.11	1502.68	2084.67	2675.47	2997.83	3519.72	4119.79
T_{off}	1.58	5.60	12.01	19.11	32.32	51.01	64.60	92.73
T_{on}	0.99	1.81	2.91	3.09	3.49	3.87	5.04	5.80
T_{on}/T_f	0.19%	0.16%	0.19%	0.15%	0.13%	0.13%	0.14%	0.14%

Finally, we analyze the computational latency of SSF-ACO-Online. Table 4 reports the duration of UAV flights T_f under online problem, along with the computation time of SSF-ACO-Online T_{on}, and that of SSF-ACO T_{off} in the corresponding offline problem. Across varying numbers of sensors, the computation times of SSF-ACO-Online stay under 6 seconds and constitute no more than 0.19% of the corresponding UAV flight duration. This demonstrates the suitability of SSF-ACO-Online for online applications. Since the active sensor list only maintains those sensors that have been discovered but not yet completely collected, though invoked SSF-ACO multiple times, SSF-ACO-Online has a cumulative computation time significantly shorter than that of SSF-ACO.

Comment 3.5

The paper uses multiple important symbols, but a comprehensive table of symbols and definitions is missing. Adding such a table would enhance readability and help readers locate information more easily.

Response 3.5:

Thanks you for the suggestion. We have added more important symbols and definitions in Table 1 in the manuscript to make it more comprehensive. The revised version is presented in Table 3 below.

Table 3: Major notations

Notation	Explanation
D	The destination point.
s_i	i-th sensor.
h_j	j-th altitude.
$l_i, l_{i,h}$	Entering boundary point of s_i.
$r_i, r_{i,h}$	Exiting boundary point of s_i.
R_i	Transmission rate of s_i.
t_i	Required transmission duration of s_i.
$\mathbb{S}$	Data structure including all sensor information.
$f(d)$	The time when UAV reaching position d.
$v, v(d)$	Speed of UAV at position d.
$g(d)$	Altitude of UAV at position d.
$p(v)$	UAV power consumption at forward speed v.
E_f	Horizontal energy consumption of UAV.
E_v	Vertical energy consumption of UAV.
E	Total energy consumption of UAV.
b_k	k-th boundary point.
C_k	k-th cell, $C_k = (b_k, b_{k+1})$.
$U_S(i)$	$= 0$, sensor s_i is inactive; $= 1$, s_i is active.
$U_C(k)$	$= 0$, cell C_k is unavailable; $= 1$, C_k is available.
$S[k, k']$	$= (b_k, b_{k'})$, path interval between b_k and $b_{k'}$.
$D[k, k']$	Effective distance of $S[k, k']$.
$T[k, k']$	Effective time of $S[k, k']$.

Comment 3.6

The discussion of related work is not sufficient. Please include recent literature on "the fusion of AI, UAV, and LAE" and provide further discussion.

Response 3.6:

Thanks for the comment. We have strengthened our manuscript in two places.

- **Section 1**: We added a summary of UAV applications in the LAE to further elucidate the indispensable role of UAVs.

- **Section 2.3**: We expanded the discussion of AI techniques applied to UAV-assisted systems.

The revised passages in Section 1 and Section 2.3 are shown below.

> UAVs, with their superior maneuverability, rapid deployment capabilities, and adaptive flight patterns, are indispensable to the LAE. They have been deployed for a wide range of applications, including last-mile package delivery [8], simultaneous localization and mapping [9], and forestry [10], [11]. When equipped with onboard processing units, UAVs can serve as mobile servers, providing computational services to ground user or vehicles [1], [12]–[14], which supply temporary computing support and alleviating computational loads.

> Learning-based methods, particularly deep learning (DL) and RL, gained popularity in recent years, as they learned complex parameters or action policies during the training process. In UAV-assisted mobile edge computing systems, Lin *et al.* [13] proposed a parametrized dueling deep Q-network to maximize the UAV's energy efficiency. The problem was formulated as a mixed-integer nonlinear programming (MINLP) problem, which facilitated the modeling of problems involving both continuous variables (*e.g.,* trajectory) and discrete variables (*e.g.,* data collection decision and task offloading decision). To maximize the total throughput and energy efficiency, Chen *et al.* [15] formulated long-term UAV-aided data collection problem as a Markov Decision Process (MDP), and addressed it by a multi-agent DRL algorithm. However, the maximum number of ground nodes that could be served in [13] and [15] was only 6 and 8, respectively, as the extremely high computational complexity became unacceptable when the number of ground nodes increased. Hao *et al.* [16] formulated a task offloading problem in a UAV-assisted mobile edge computing system as a MINLP, and then transformed it into a MDP. The problem was solved by a DRL algorithm. Zhong *et al.* [17] also applied a similar approach to address a task offloading and resource allocation problem. Despite their successful application to larger-scale problems, challenges still remain in the context of the JUSAS problem, particularly in modeling the environment and designing the reward function, including aligning the reward signal with the objective and dealing with sparse rewards.

[1] G. Sun, L. He, Z. Sun, *et al.*, "Joint Task Offloading and Resource Allocation in Aerial-Terrestrial UAV Networks With Edge and Fog Computing for Post-Disaster Rescue," *IEEE Trans. Mobile Comput.*, vol. 23, no. 9, pp. 8582–8600, 2024.

[2] Y. Zeng, J. Xu, and R. Zhang, "Energy minimization for wireless communication with rotary-wing UAV," *IEEE Trans. Wireless Commun.*, vol. 18, no. 4, pp. 2329–2345, 2019.

[3] L. Zhang, Z.-Y. Zhang, L. Min, *et al.*, "Task Offloading and Trajectory Control for UAV-Assisted Mobile Edge Computing Using Deep Reinforcement Learning," *IEEE Access*, vol. 9, pp. 53 708–53 719, 2021.

[4] L. He, G. Sun, Z. Sun, *et al.*, "An Online Joint Optimization Approach for QoE Maximization in UAV-Enabled Mobile Edge Computing," in *IEEE INFOCOM 2024 - IEEE Conf. Comput. Commun.*, IEEE, 2024, pp. 101–110.

[5] Z. Sun, G. Sun, L. He, F. Mei, S. Liang, and Y. Liu, "A Two Time-Scale Joint Optimization Approach for UAV-assisted MEC," in *IEEE INFOCOM 2024 - IEEE Conf. Comput. Commun.*, IEEE, 2024, pp. 91–100.

[6] X. Dai, Z. Xiao, H. Jiang, and J. C. S. Lui, "UAV-Assisted Task Offloading in Vehicular Edge Computing Networks," *IEEE Trans. Mobile Comput.*, vol. 23, no. 4, pp. 2520–2534, 2024.

[7] L. Fu, Z. Zhao, G. Min, W. Miao, L. Zhao, and W. Huang, "Energy-Efficient 3-D Data Collection for Multi-UAV Assisted Mobile Crowdsensing," *IEEE Trans. Comput.*, vol. 72, no. 7, pp. 2025–2038, 2022.

[8] S. Wandelt, S. Wang, C. Zheng, and X. Sun, "AERIAL: A Meta Review and Discussion of Challenges Toward Unmanned Aerial Vehicle Operations in Logistics, Mobility, and Monitoring," *IEEE Trans. Intell. Transp. Syst.*, vol. 25, no. 7, pp. 6276–6289, 2024.

[9] M. Karrer and M. Chli, "Distributed Variable-Baseline Stereo SLAM from two UAVs," in *2021 IEEE Int. Conf. Robot. and Automat. (ICRA)*, 2021, pp. 82–88.

[10] G. Sun, X. Zheng, J. Li, H. Kang, and S. Liang, "Collaborative WSN-UAV Data Collection in Smart Agriculture: A Bi-objective Optimization Scheme," *ACM Trans. Sensor Netw.*, 2023.

[11] C. Dalai, M. Singh, A. S. Kumara, W. Patel, H. Patil, and R. Maranan, "Monitoring Water Levels in Rivers with optical fiber sensors," in *2024 5th Int. Conf. Innovative Trends in Inf. Technol. (ICITIIT)*, IEEE, 2024, pp. 1–6.

[12] X. Dai, Z. Xiao, H. Jiang, and J. C. S. Lui, "UAV-Assisted Task Offloading in Vehicular Edge Computing Networks," *IEEE Trans. Mobile Comput.*, vol. 23, no. 4, pp. 2520–2534, 2024.

[13] N. Lin, H. Tang, L. Zhao, S. Wan, A. Hawbani, and M. Guizani, "A PDDQNLP algorithm for energy efficient computation offloading in UAV-assisted MEC," *IEEE Trans. Wireless Commun.*, vol. 22, no. 12, pp. 8876–8890, 2023.

[14] Y. Liao, Y. Song, S. Xia, Y. Han, N. Xu, and X. Zhai, "Energy Minimization of RIS-Assisted Cooperative UAV-USV MEC Network," *IEEE Internet of Things J.*, vol. 11, no. 20, pp. 32 490–32 502, 2024.

[15] G. Chen, X. B. Zhai, and C. Li, "Joint optimization of trajectory and user association via reinforcement learning for UAV-aided data collection in wireless networks," *IEEE Trans. Wireless Commun.*, vol. 22, no. 5, pp. 3128–3143, 2022.

[16] H. Hao, C. Xu, W. Zhang, S. Yang, and G.-M. Muntean, "Joint Task Offloading, Resource Allocation, and Trajectory Design for Multi-UAV Cooperative Edge Computing With Task Priority," *IEEE Trans. Mobile Comput.*, vol. 23, no. 9, pp. 8649–8663, 2024.

[17] L. Zhong, Y. Li, M.-F. Ge, M. Feng, and S. Mao, "Joint Task Offloading and Resource Allocation for LEO Satellite-Based Mobile Edge Computing Systems With Heterogeneous Task Demands," *IEEE Trans. Veh. Technol.*, 2025, early access.